Brittle Bacteria: A Biomimetic Approach to the Formation of Fibrous Composite Materials

Sean A. Davis,[†] Harish M. Patel,[†] Eric L. Mayes,[†] Neil H. Mendelson,[‡] Gabriella Franco,[†] and Stephen Mann*[,†]

Department of Chemistry, University of Bath, Bath, BA2 7AY, U.K., and Department of Molecular and Cellular Biology, University of Arizona, Tucson, Arizona 85721

Received April 16, 1998. Revised Manuscript Received July 2, 1998

Organized bacterial superstructures have been used as 3-D templates for the fabrication of ordered inorganic−organic fibrous composites. Preformed magnetic (Fe_3O_4) and semiconducting (CdS) inorganic nanoparticles were incorporated into macroscopic threads of *Bacillus subtilis* by reversible swelling of the superstructure in colloidal sols. The air-dried mineralized fibers consisted of a closely packed array of 0.5 μm diameter multicellular bacterial filaments, each of which was coated with a 30−70 nm thick layer of aggregated colloidal particles. Inorganic patterning of the interfilament spaces was influenced by the surface charge of the nanoparticles used. Whereas negatively charged magnetite colloids gave good infiltration and replication of the bacterial superstructure, the neutral-ligand-capped CdS colloid, although internalized to some extent, was preferentially localized at the surface of the thread. Positively charged sols of TiO_2, in contrast, did not penetrate the swollen fiber but produced coherent surface coatings of uniform thickness. Attempts to pattern the deposition of CdS using molecular precursors by exposing a Cd(II)-containing bacterial fiber to H_2S gas produced an uneven surface coat of CdS particles. Removal of the bacterial component from the magnetic composite by heating at elevated temperatures resulted in structural collapse.

Introduction

A central objective of biomimetic materials chemistry is to develop new strategies for the synthesis of materials and composites that exhibit the organizational and functional specificity exemplified by biological minerals such as bones, shells, and teeth.[1,2] Some progress has been made toward developing biomimetic approaches to the formation of inorganic materials with controlled size, shape, orientation, and polymorphic structure.[3,4] Current research is also investigating routes to the synthesis of inorganic materials with complex form[5,6] and higher-order hybrid assemblies,[7−10] often reminiscent of the hierarchical structures seen in nature. A generic approach to these biomimetic materials involves the inorganic replication of a preformed organic assembly possessing an extended and patterned architecture. In this paper we develop this strategy by using a bacterial template with reversible swelling properties to fabricate fibrous bioinorganic composites consisting of organized arrays of magnetic or semiconducting nanoparticles.

Bacterial threads can be produced from a mutant strain of the bacterium *Bacillus subtilis*, which has a cylinder-shaped cell, 0.8 μm in diameter and 4 μm in length. In fluid cultures, the mutant strain, which exhibits suppressed cell separation, can only grow by elongation at constant diameter along the cylinder axis to produce long multicellular filaments that intertwine to form weblike structures (Figure 1). Drawing these web structures from the culture medium results in compaction of the individual filaments at the fluid−air interface to give a macroscopic bacterial thread, often several decimeters long and 0.1−0.2 mm wide.[11,12] The air-dried thread consists of a superstructure of multicellular filaments aligned parallel to the thread axis and arranged in a pseudohexagonal-packed configuration, reminiscent of the organization of cylindrical surfactant micelles in the H_I liquid−crystal lyotropic phase, albeit on a length scale 2 orders of magnitude greater. A

* To whom correspondence should be addressed.
[†] University of Bath.
[‡] University of Arizona

(1) Sarikaya, M.; Aksay, I. A. *Biomimetics: Design and Processing of Materials;* AIP Series in Polymers and Complex Materials; AIP Press: New York, 1995.
(2) Mann, S. *Biomimetic Materials Chemistry*; VCH Publishers: New York, 1996.
(3) Mann, S. *J. Mater. Chem.* **1995**, *5*, 935.
(4) Heuer, A. H.; Fink, D. J.; Laraia, V. J.; Arias, J. L.; Calvert, P. D.; Kendall, K.; Messing, G. L.; Blackwell, J.; Rieke, P. C.; Thompson, D. H.; Wheeler, A. P.; Veis, A.; Caplan, A. I. *Science* **1992**, *255*, 1098−1105.
(5) Mann, S.; Ozin, G. A. *Nature* **1996**, *382*, 313−318.
(6) Mann, S. *J. Chem. Soc., Dalton Trans.* **1997**, 3953.
(7) Aksay, I. A.; Trau, M.; Manne, S.; Hunma, I.; Yao, N.; Zhou, L.; Fenter, P.; Eisenberger, P. M.; Gruner, S. M. *Science* **1996**, *273*, 892.
(8) Antonietti, M.; Göltner, C. *Angew. Chem., Int. Ed. Engl.* **1997**, *36*, 910.
(9) Mann, S.; Burkett, S. L.; Davis, S. A.; Fowler, C. E.; Mendelson, N. H.; Sims, S. D., Walsh, D.; Whilton, N. T. *Chem. Mater.* **1997**, *9*, 2300.
(10) Combs, N.; Khushalani, D.; Oliver, S., Ozin, G. A.; Shen, G. S.; Sokolov, I.; Yang, H. *J. Chem. Soc., Dalton Trans.* **1997**, 3941.
(11) Mendelson, N. H.; Thwaites, J. J. *MRS Symp. Proc.* **1990**, *174*, 171.
(12) Thwaites, J. J.; Mendelson, N. H. *Proc. Natl. Acad. Sci. U.S.A.* **1985**, *82*, 2163.

S0897-4756(98)00285-3 CCC: $15.00
Published on Web 08/29/1998

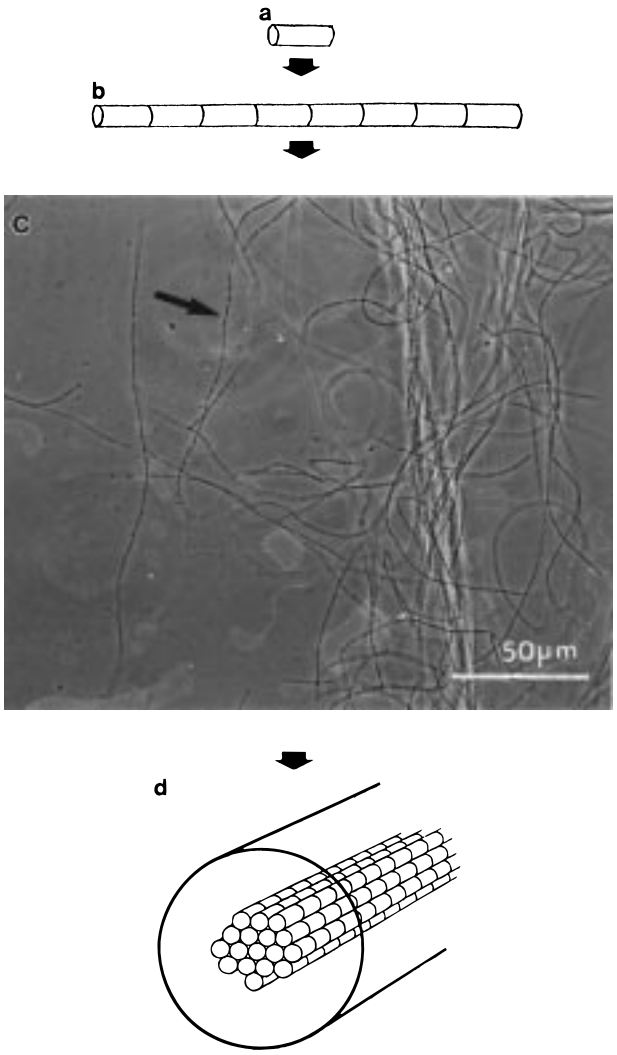

Figure 1. Different levels of cellular organization in bacterial thread. (a) individual rod shaped cells of *B. subtilis*, (b) growth at constant diameter to produce multicellular filaments, (c) optical micrograph of cultured bacteria showing intertwined filaments with weblike structures, and (d) withdrawing of multicellular filaments through the air−water interface produces macroscopic bacterial thread with organized internal superstructure.

typical bacterial thread can contain in excess of 10^{10} cells and 50 000 filaments arranged as a cell → filament → thread hierarchy of cylindrical building units.[13]

The strong metal-binding ability of the cell wall of *B. ubtilis*[14] has been utilized for the mineralization of multicellular bacterial filaments prior to drawing of the macroscopic composite fiber.[15] For example, addition of soluble metal salts of iron and calcium directly to unwashed web cultures resulted in the formation of precipitates on the filaments within the web culture.[16] Analysis of fibers drawn from these mineralized web structures indicated a metal content of 10−16 wt % deposited in the form of mineral phases such as Fe_2O_3 and $CaCO_3$. However, no precipitation was observed on the filaments prior to drawing into a fiber when washed webs or copper salts were used. The corresponding drawn fibers contained mineral deposits formed by solution evaporation, but the metal loadings were significantly reduced. The internal microstructure of the composite fibers produced from mineralized webs (both washed and unwashed) was not systematically studied.

In recent studies, we have been investigating an alternative method to the fabrication of organized bacterial−mineral composites that is based on reversible swelling of unmineralized threads in the presence of preformed inorganic nanoparticles.[17] Our objective is to exploit the underlying organization of the thread as a template for producing composites with an extended, ordered microstructure. This was achieved by loading the bacterial thread with colloidal suspensions of ceramic nanoparticles, followed by air-drying to consolidate the inorganic mineral and to replicate the interfilament spaces in the form of a continuous inorganic framework. Moreover, removal of the bacterial template by calcination produced a silica fiber with ordered macroporous channels. We also infiltrated the organic superstructure with a colloidal dispersion of a surfactant-templated mesostructured silica phase (MCM-41) to illustrate how bacterial templates could be used in hierarchical processing. An ordered macroporous fiber with channel walls of periodic mesoporous silica was obtained after calcination.[17] Here we describe the use of a preformed bacterial thread for the production of fiberlike composites containing Fe_3O_4, CdS, or TiO_2 nanoparticles.

Experimental Section

Production of Bacterial Thread. The cultures of *B. subtilis* strain FJ7(II) were grown at 20 °C in 100 mm diameter plastic Petri dishes containing 16 mL of tryptose blood (TB) medium, consisting of tryptose (10 g/L), beef extract (3 g/L), and NaCl (5 g/L), supplemented with uracil (20 mg/L).[18] Decimeter-long bacterial threads were produced by slowly pulling the web from solution using a thin wire hook, withdrawn at 22 mm min^{-1} by a rate-controlled motor, and were left to dry in air.

Synthesis of Magnetite (Fe_3O_4) Nanoparticles. A magnetite colloid was prepared in alkaline media according to the general procedure described elsewhere.[19] An aqueous solution containing iron(III) chloride hexahydrate (4 mL, 0.0085 mol) and ammonium iron(II) sulfate hexahydrate (1 mL, 0.0043 mol, in 2 M HCl) was added to 50 mL of 1 M tetramethylammonium hydroxide. The resulting black suspension was stirred for 1 h at room temperature and then placed in an ultrasonic bath for 1 h. The colloid produced was centrifuged at 20 000*g* for 1 h. The supernatant was decanted and the sediment resuspended in 20 mL of water by sonication. The black dispersion obtained was filtered through a 0.2 μm pore cellulose nitrate membrane filter. The particle size of the approximately spherical particles was 9.1 ± 2.4 nm as determined by transmission electron microscopy. Electron diffraction data [d_{hkl} = 0.500 nm (111), 0.305 nm (220), 0.259 nm (311), 0.216 nm (400)] were consistent with magnetite.

Synthesis of Cadmium Sulfide (CdS) Nanoparticles. A CdS colloid was prepared by the following procedure:[20] cadmium acetate (2.712 g, 0.0118 mol), thiourea (0.263 g, 0.00346 mol), and 3-mercapto-l,2-propanediol (0.945 cm^3,

(13) Mendelson, N. H.; Thwaites, J. J. *J. Bacteriol.* **1989**, *171*, 1055.
(14) Beveridge, T. J.; Murray, R. G. E. *J. Bacteriol.* **1976**, *127*, 1502.
(15) Mendelson, N. H. *Science* **1992**, *258*, 1633.
(16) Mendelson, N. H.. In *Biomimetic Materials Chemistry*; Mann, S., Ed.; VCH Publishers: New York, 1996; pp 279−313.
(17) Davis, S. A.; Burkett, S. L.; Mendelson, N. H.; Mann, S. *Nature* **1997**, *385*, 420.
(18) Mendelson, N. H. *Proc. Natl. Acad. Sci. U.S.A.* **1976**, *73*, 1740.
(19) Massart, R. *IEEE Trans. Magnet.* **1981**, *17*, 1247.
(20) Chemseddine, A.; Feaheiley, M. L. *Thin Sol. Films* **1994**, *247*, 3.

0.0113 mol) were mixed together with dimethylformamide (200 cm^3) for approximately 1 h, under a flow of argon. The mixture was then heated to 100−130 °C for 20 min and allowed to cool for 30 min. This heating−cooling cycle, which decomposes the thiourea and generates S^{2-} ions, was repeated, and on the third heating cycle, a white precipitate of CdS formed. The precipitate was isolated by centrifugation, washed with acetone followed by diethyl ether (to remove residual Cd(II) ions), and finally dried in vacuo. The particle diameter determined by TEM was 3.4 ± 0.7 nm. XRD measurements of films and powders prepared from the dispersion indicated that the CdS nanoparticles adopt the ZnS blende structure [$d_{hkl} = 0.336$ nm (111), 0.290 nm (200), 0.206 nm (220), 0.175 nm (311)].

Synthesis of Titania (TiO_2) Colloid. Colloidal titania was prepared by hydrolysis of titanium tetraisopropoxide under a nitrogen atmosphere using the procedure described previously.[21] Titanium(IV) isopropoxide (1.25 mL, 0,00424 mol) was added to 0.25 mL of 2-propanol in a syringe. This mixture was added dropwise over 5 min to 10 mL of distilled, deionized water while the mixture stirred vigorously. Ten minutes after the final alkoxide addition, 0.05 mL of 70% nitric acid was added. The hydrolysis mixture was then stirred for 8 h at 80 °C to remove the 2-propanol. The mean particle diameter from TEM studies was 8.2 ± 2.2 nm. Electron diffraction indicated that the major phase present was the anatase polymorph of TiO_2 [$d_{hkl} = 0.355$ nm (101), 0.238 nm (004), 0.231 nm (112), 0.191 nm (200), 0.169 nm (105)]. A small amount of brookite, also a polymorph of TiO_2, was also detected [$d_{hkl} = 0.292$ nm (121)].

Preparation of Mineralized Bacterial Composites from Preformed Nanoparticles. Fiber composites were prepared by dipping 5 cm long samples of prewashed bacterial thread into a colloidal dispersion of inorganic nanoparticles (Fe_3O_4, CdS, or TiO_2) for between 5 and 120 min. Samples were then carefully removed from the colloid-containing solution and allowed to dry in air for at least 24 h prior to analysis. Reverse tweezers were used to hold the bacterial thread throughout the process. During the dipping process, the tweezers were held so that the tip was not immersed in the dispersion, and the portion of bacterial thread being held remained dry, which aided the recovery of the composite fiber. Consequently, a portion of the loaded thread remained bare and this was removed from the air-dried samples before further analysis.

A portion of a magnetite−bacterial thread composite was placed in a crucible and heated in air to 600 °C in an oven. The temperature was increased in 50 °C increments at 30 min intervals. The oven was turned off after 2 h and allowed to cool to room temperature before the product was recovered.

Preparation of Mineralized Bacterial Composites by in Situ Deposition. A 5 cm long portion of a prewashed bacterial thread was dipped into a 1.0 M cadmium chloride solution for 2 h, redrawn, and allowed to dry in air overnight. The Cd-containing bacterial thread was then placed in a desiccator and exposed to a constant supply of H_2S, generated from the reaction of Na_2S(s) with HCl(aq), for 7 days.

Characterization. Scanning electron microscopy (SEM) and energy-dispersive X-ray analysis (EDXA) were performed using a JEOL 6310 SEM operated at 15 keV. Samples were prepared for analysis using one of two different methods. First, air-dried uncoated samples were mounted onto aluminum stubs using circular carbon adhesive pads for EDX analysis and then gold-coated in an Edwards S150B sputter-coater for 4 min for imaging studies. Second, resin-embedded samples were mounted onto aluminum stubs using a carbon "gum" and gold-coated for 2 min, after which a carbon paste was applied between the gold coat and the stub to enhance the electrical conductivity of the resin blocks. Elemental distribution maps were generated by EDX analysis and corresponding secondary electron images obtained.

(21) O'Regan, B.; Moser, J.; Anderson, M.; Gratzel, M. *J. Phys. Chem.* **1990**, *94*, 8720.

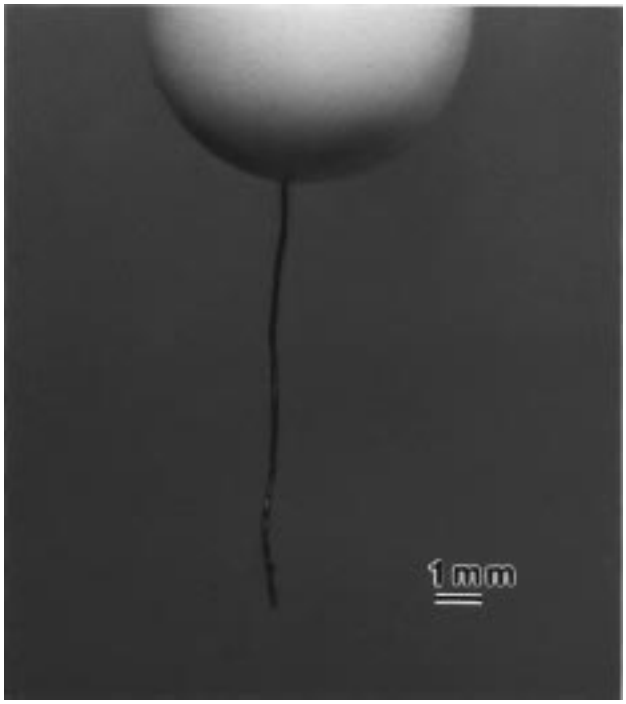

Figure 2. A bacterial−magnetite fibrous composite attracted to and vertically suspended from a permanent bar magnet.

Thin sections of the composite fibers were prepared for transmission electron microscopy (TEM) analysis by dehydrating a 1 cm length of the material for 1 h in 50 mL of 50:50 MeOH/H_2O containing 0.5 mL of silane to aid adhesion between the sample and resin. After drying in air for 90 min, the fiber was transferred to a sample bottle, covered in TAAB hard resin, and placed in a rotator for at least 12 h to allow infiltration of the resin into the fiber. The sample was then placed in an embedding mold and covered with fresh resin, which was polymerized in an oven at 60 °C for 2 days. Sections were prepared using a diamond knife on an OMU3 ultramicrotome. Thin sections were cut perpendicular to the fiber axis to a thickness of typically 50−100 nm (silver−gold interference colors). Sections were collected on Formvar-covered, carbon-coated, 3 mm slotted copper grids and left unstained. TEM imaging, selected area electron diffraction studies, and EDXA were performed on a JEOL 2000FX analytical TEM operated at an accelerating voltage of 200 keV.

X-ray diffraction data were recorded from whole samples, using a Phillips X-ray powder diffractometer with Cu Kα (l = 1.5405 Å) radiation.

Results

Bacterial−Magnetite Fibrous Composites. Dipping of bacterial threads into a ferrofluid of magnetite nanoparticles resulted in visible swelling of the biological superstructure without loss of structural integrity. The swollen fiber was withdrawn through the air−liquid interface to produce a compact black fiber that was initially pliable due to its high moisture content. Drying in air gave a consolidated, brittle fiber of similar size to the unmineralized bacterial thread. The iron loading in the dried sample was 19 wt %, as determined by atomic absorption spectrometry. The mass loading of magnetite in the composite was calculated as 26 wt %, by assuming a chemical composition of Fe_3O_4. The composite fibers were sufficiently magnetic that they responded and tracked to an external magnetic field and could be suspended vertically under the poles of a bar magnet (Figure 2). Further details on the superpara-

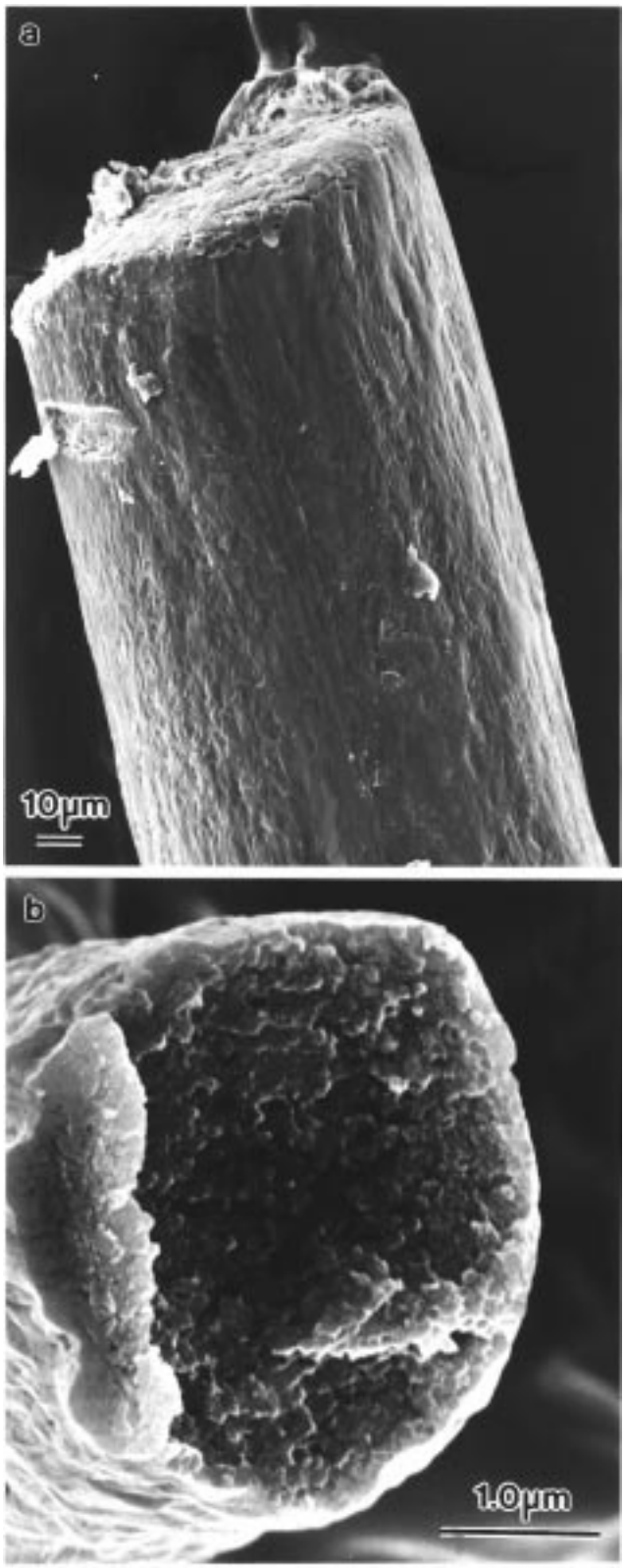

Figure 3. SEM images of (a) the external surface and (b) cross section of a bacterial−magnetite fibrous composite.

magnetic properties of the composite fibers are reported elsewhere.[22]

The surface and internal texture of the individual composite fibers (Figure 3) was significantly different than that of the unmineralized bacterial thread. A thin mineral coating, which gave peaks for iron by energy-dispersive X-ray analysis (data not shown), obscured the underlying bacterial cells. The fibers appeared uniformly dark in cross section, indicating that the mineral phase was not restricted to the surface of the fiber. This was confirmed by mapping the iron distribution of a sample in cross section (Figure 4), as well as TEM imaging of the central region of thin transverse sections (Figure 5). The TEM data showed that discrete magnetite nanoparticles were concentrated around and between the multicellular filaments of the bacterial superstructure to produce an extended and interconnected microskeletal framework. The thickness of the mineral walls was typically between 50 and 70 nm.

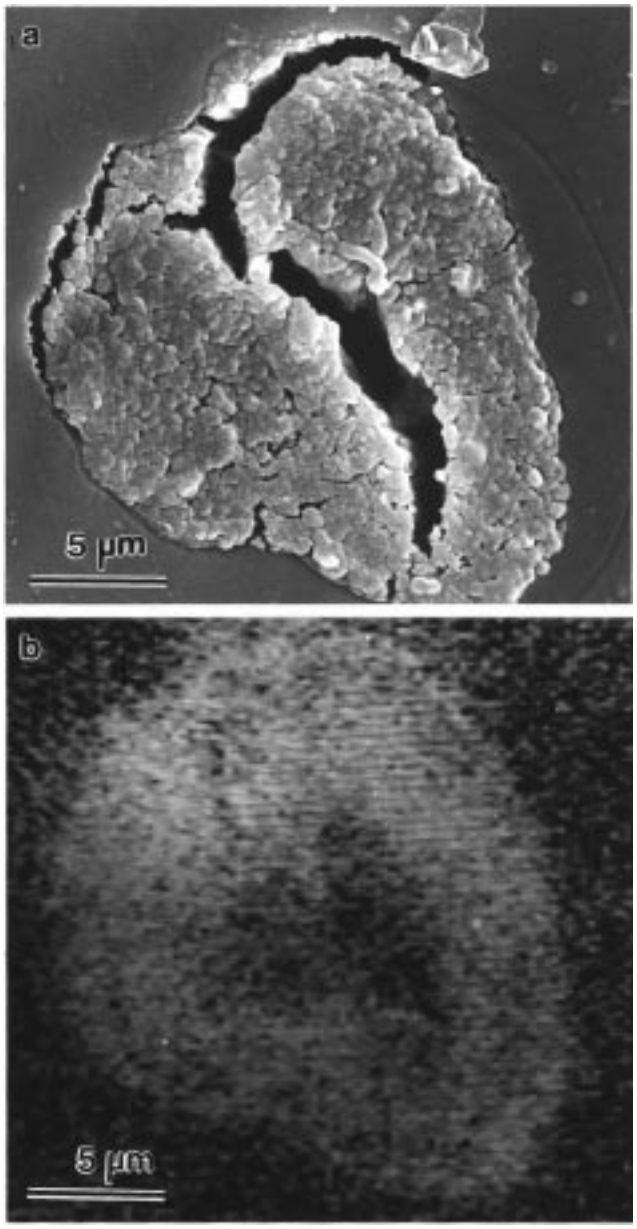

Figure 4. (a) SEM image of a resin-embedded bacterial−magnetite composite imaged in cross section. (b) Corresponding elemental distribution map for iron.

Removal of the bacterial template by high-temperature curing produced an intact but extremely brittle black fiber. Any attempt to manipulate the sample resulted in collapse of the structure.

(22) Smith, C. J.; Field, M.; Coakley, C. J.; Awschalom, D. D.; Mendelson, N. H.; Mayes, E. L.; Davis, S. A.; Mann, S. *IEEE Trans. Magn.* **1998**, *34*, 988.

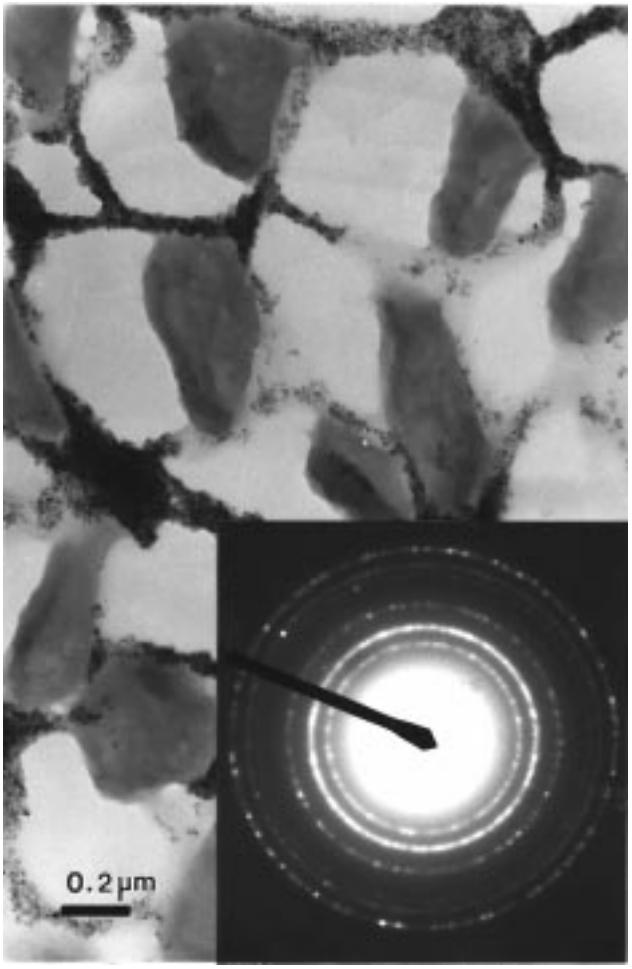

Figure 5. TEM image of a transverse thin section of a bacterial−magnetite composite fiber showing aggregated Fe_3O_4 nanoparticles (darkest areas in the micrograph) within the interfilament spacings. Inset: associated selected-area diffraction patterns confirming the presence of magnetite [d_{hkl} = 0.492 nm (111), 0.300 nm (220), 0.253 nm, 0.212 nm].

Bacterial−CdS Fibrous Composites. Dipping bacterial thread into an aqueous suspension of CdS nanoparticles produced a fiber that was not significantly different than the original bacterial thread in appearance. SEM microscopy of the composite fiber revealed that the fiber surface consisted of partially disorganized filaments and discrete, randomly distributed micron-scale mineral aggregates (Figure 6), which contained Cd and S (EDX data not shown). Thus, the CdS colloid produced localized aggregates rather than a uniform coating of the fiber surface. However, elemental mapping indicated that the inorganic phase was dispersed throughout the bacterial thread (Figure 7), although a higher concentration was observed near to the edge of the fiber due to the surface aggregates. TEM micrographs of transverse thin sections (Figure 8) showed that the bacterial filaments were comparatively well-ordered in the center of the fiber, in contrast to their surface organization. Higher magnification images (Figure 8b) revealed 30−40 nm thick electron dense regions surrounding individual filaments that were attributed to closely packed arrays of the CdS nanoparticles. No electron diffraction patterns could be recorded from these areas due to the low localized concentration of the colloidal particles.

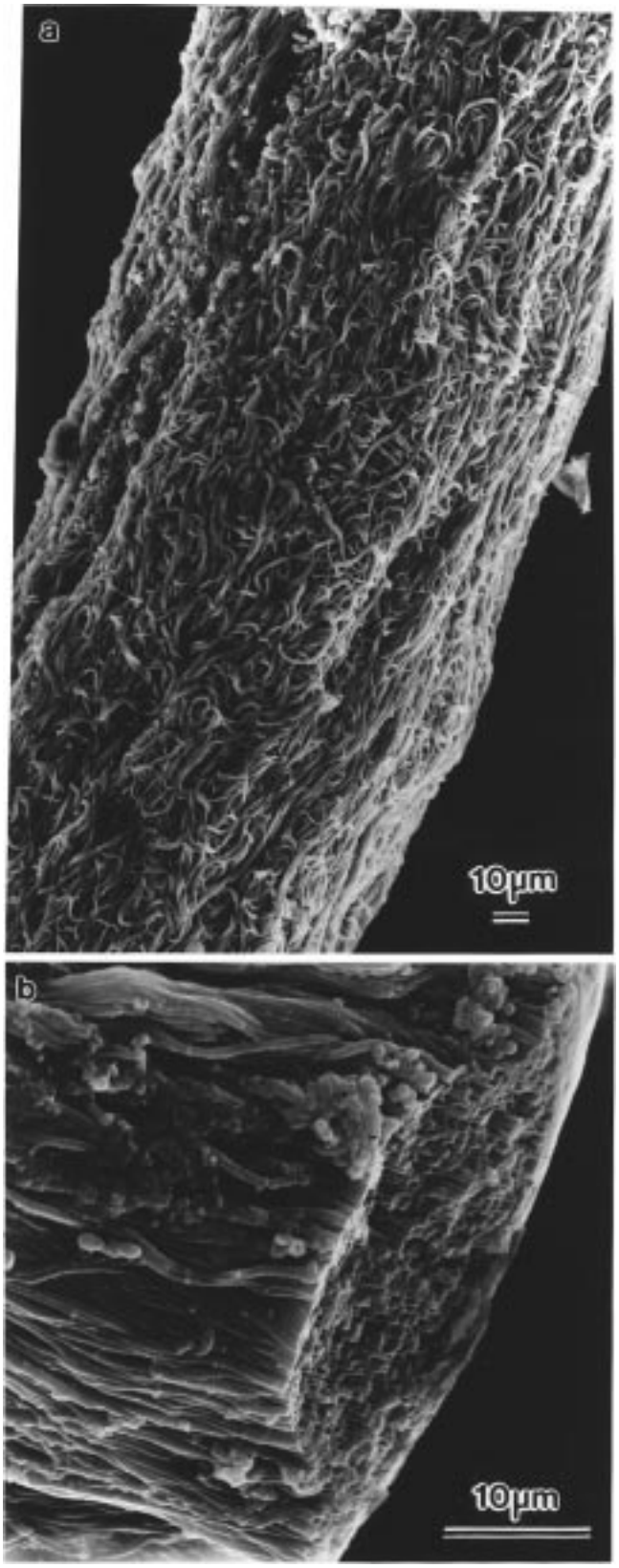

Figure 6. (a) SEM of the surface of a bacterial−CdS composite fiber. (b) Higher magnification image showing detail of a fractured surface.

In Situ Mineralization of CdS in the Bacterial Thread. Dry fibers, produced after dipping bacterial thread into aqueous $CdCl_2$ solution, were white and of similar diameter to the native material. Although Cd was detected by EDX analysis (data not shown), no

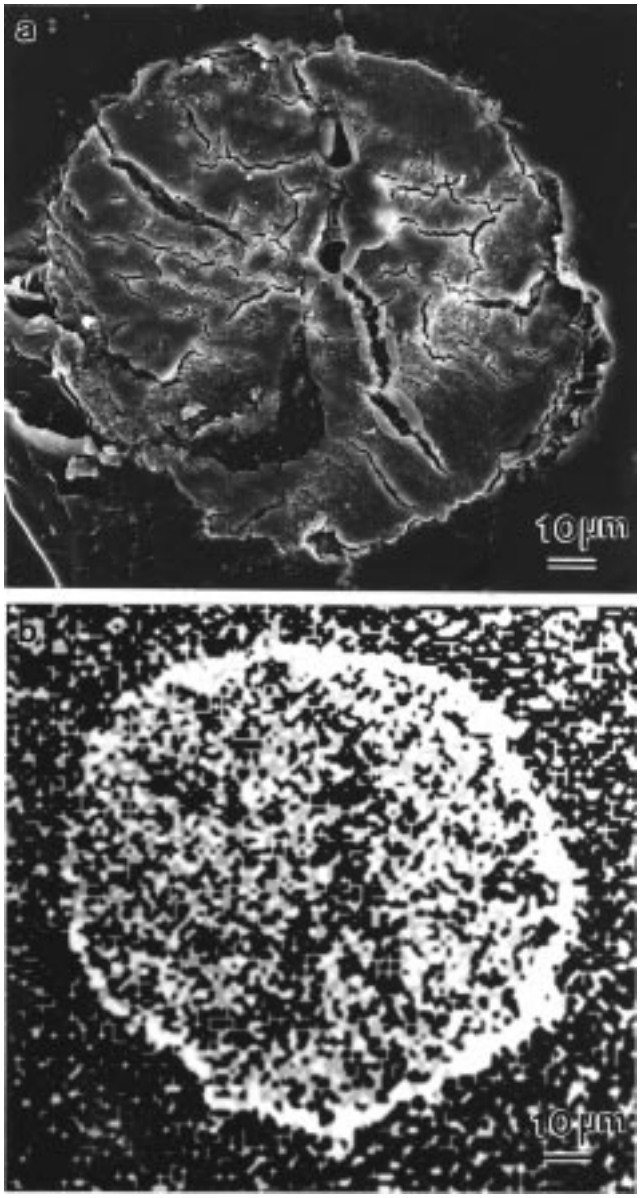

Figure 7. (a) SEM of a bacterial−CdS composite imaged parallel to the fiber axis. (b) Corresponding elemental distribution map for Cd.

mineral phases, such as a $CdCl_2$ evaporite, were observed by SEM examination of the fiber surface, which consisted of disorganized bacterial filaments. The Cd-containing bacterial thread developed a yellow coloration when exposed to H_2S. Examination of the fiber by SEM revealed an uneven surface coating which consisted of a mass of platelike, and smaller discrete crystals (Figure 9). Elemental mapping indicated that Cd and S were not evenly distributed throughout the fiber but were concentrated near the surface (Figure 10). X-ray diffraction (XRD) of the composite fiber indicated the presence of a crystalline CdS phase with the ZnS blende structure [d_{hkl} = 0.335 nm (111), 0.298 nm (200), 0.206 nm (220)]. TEM imaging of thin sections clearly showed the presence of a surface coating about 60 nm thick (Figure 11). Electron diffraction data recorded from this area were consistent with the XRD data. Cadmium sulfide particles were also identified at much lower loadings in the center of the thread by EDX analysis (data not shown).

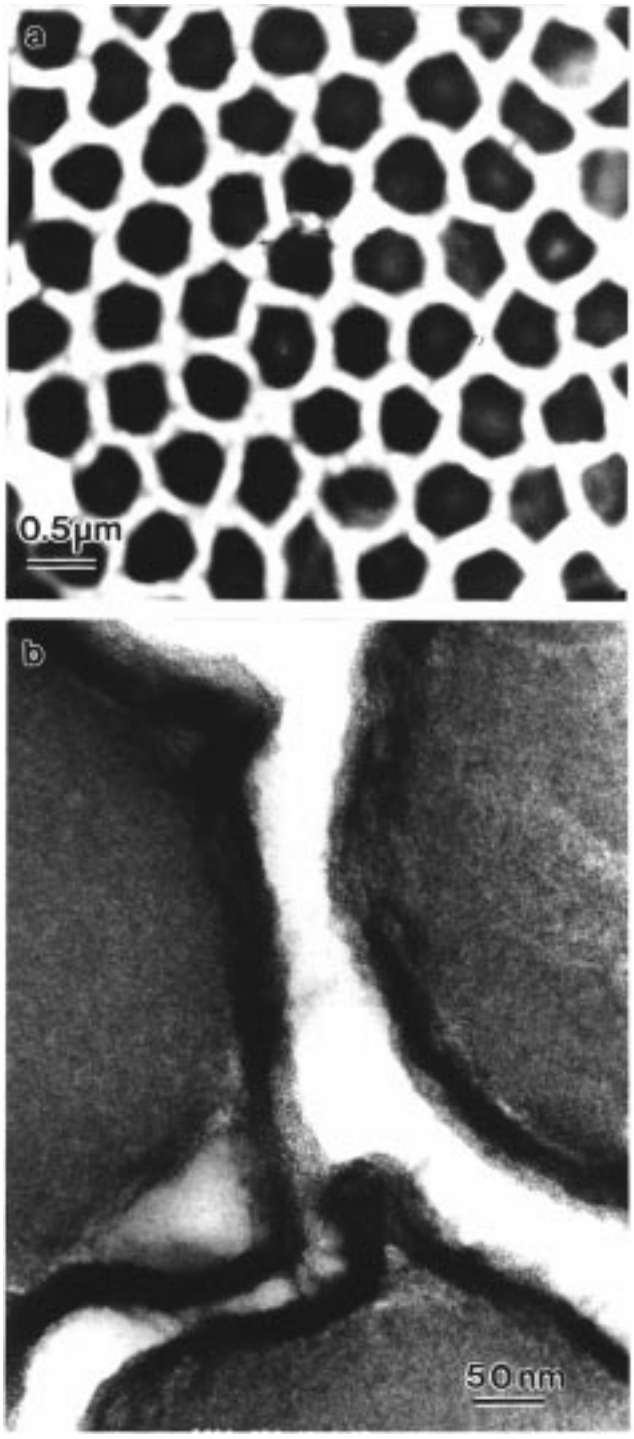

Figure 8. (a) Low-magnification TEM micrograph of a transverse thin section of a bacterial−CdS composite showing the ordered arrangement of the bacterial filaments near the center of the fiber. (b) Higher magnification image of individual bacterial filaments showing a densely packed array of CdS nanoparticles on the cell walls.

Bacterial−Titania Fibrous Composites. A pale white fiber was produced by dipping bacterial thread into an aqueous dispersion of titania nanoparticles. Examination of the surface of the fiber by SEM revealed a distinct mineral coating (Figure 12), which appeared smooth and of quite uniform thickness. The apparent platelike morphology originated from shrinkage of a thin mineral film during drying which caused extensive cracking, predominantly perpendicular and parallel to

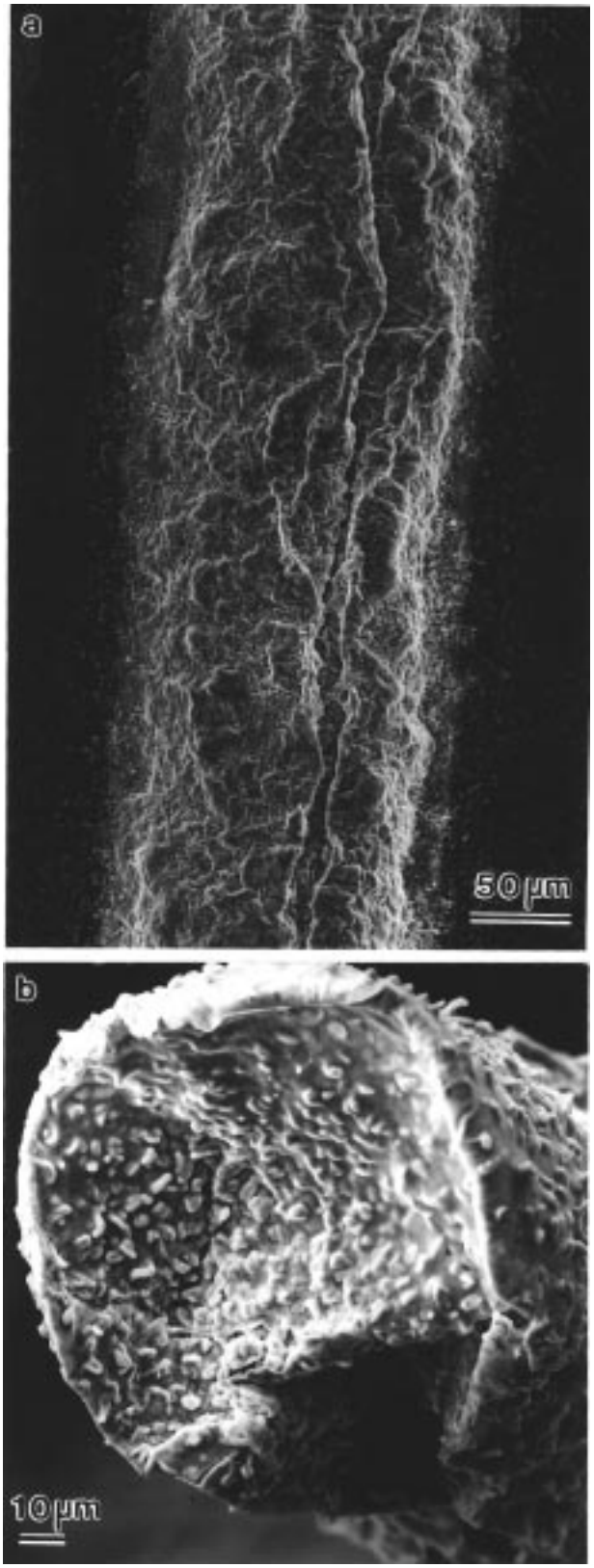

Figure 9. (a) SEM of the surface of a bacterial thread mineralized in situ with CdS. (b) Higher magnification image of the tip of a composite fiber.

the fiber axis. The characteristic texture of the underlying bacterial thread was visible between some of the mineral plates. X-ray analysis indicated the presence of Ti and P (data not shown). Lattice spacings obtained by XRD of the composite fiber were the same as those

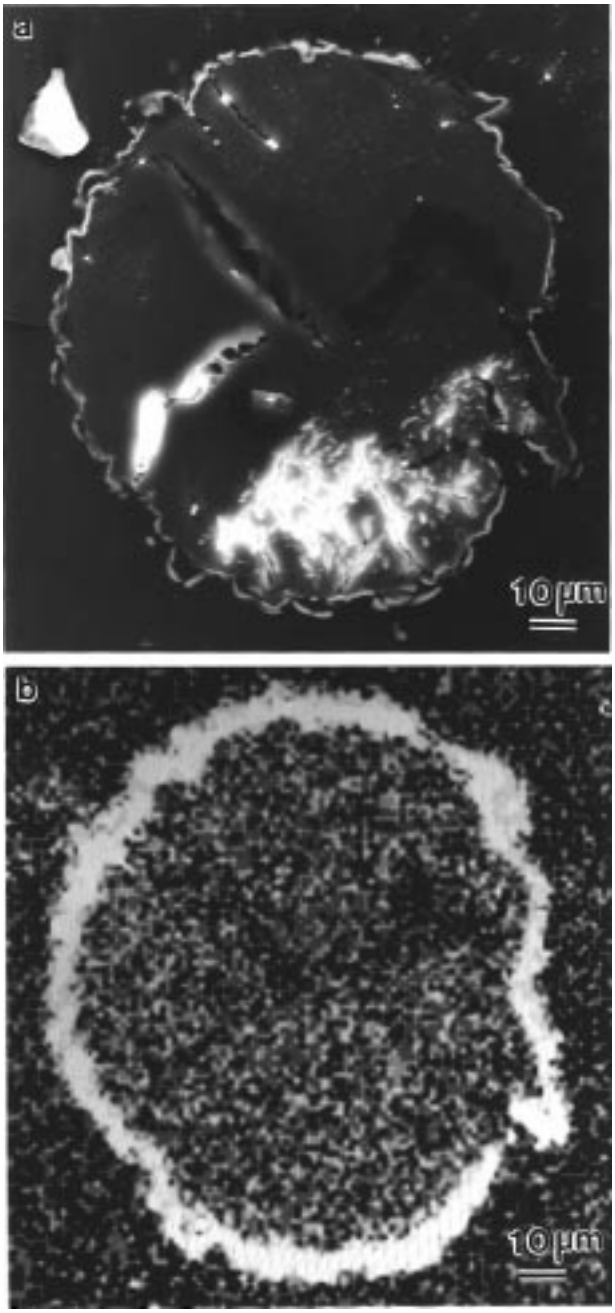

Figure 10. (a) SEM image of an in situ mineralized bacterial−CdS composite fiber viewed in cross section. (b) Corresponding elemental distribution map for S.

obtained from the TiO_2 colloid (d = 0.350 nm, 0.304 nm, 0.238 nm, 0.190 nm, 0.168 nm, 0.148 nm). The mineral phase was therefore identified as being predominantly anatase.

The distinct surface coating was clearly discernible by SEM examination of a sample in cross section (Figure 13). When compared with the corresponding elemental distribution map for titanium, it was clear that the mineral phase was present only at the surface of the macroscopic thread. No infiltration into the center of the thread was observed. The thickness of the surface coating was estimated as 0.5−5 μm. TEM studies of different regions of transverse thin sections of the fiber indicated a densely consolidated surface coat (Figure 14) and negligible infiltration of TiO_2 between the coaligned bacterial filaments.

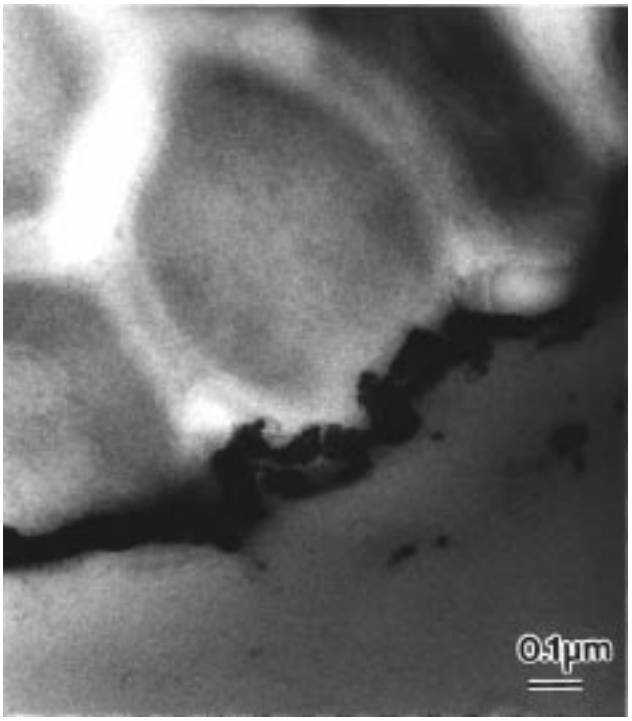

Figure 11. TEM image of the outer edge of a bacterial−CdS composite fiber mineralized in situ. The mineral phase forms a distinct surface coating.

Discussion

The technique of utilizing organic templates for the fabrication of fibrous hybrids is currently being explored in a number of systems. Often, preformed static templates are surface-coated to produce biomimetic composite materials; for example, composite magnetite−textile polyester fibers[23] and magnetic spider silk threads[24] have been prepared by absorbing magnetite particles onto the surface of the (bio)polymers. Similarly, hollow ceramic cylinders have been fabricated by calcining silica-[25] or aluminum hydroxide-coated[26] phospholipid tubules.

In contrast, the work described here illustrates that organized organic superstructures with reversible swelling properties can be exploited in the preparation of mineral-infiltrated fibrous composites, provided that the surface charge of the inorganic phase is appropriately tailored. The bacterial filaments are negatively charged due to the predominance of carboxylate groups on the cell membrane. Thus, colloids with a net positive surface charge, such as TiO_2, tend to deposit only on the external surface of the macroscopic bacterial thread, to give uniform coatings, whereas a negatively charged colloid, such as magnetite or silica,[17] penetrates into the interior of the thread to produce an organized inorganic phase that is patterned within the interspaces between the multicellular filaments. Presumably in this case, repulsive forces between the nanoparticles and cell membranes give rise to good infiltration and swelling when the superstructure comes into contact with sol. The extent of infiltration of the CdS nanoparticles was less than that observed for the magnetite colloid but greater than for the TiO_2 system, which is consistent with the presence of uncharged polar hydroxylated ligands on the surface of the CdS nanocrystals.

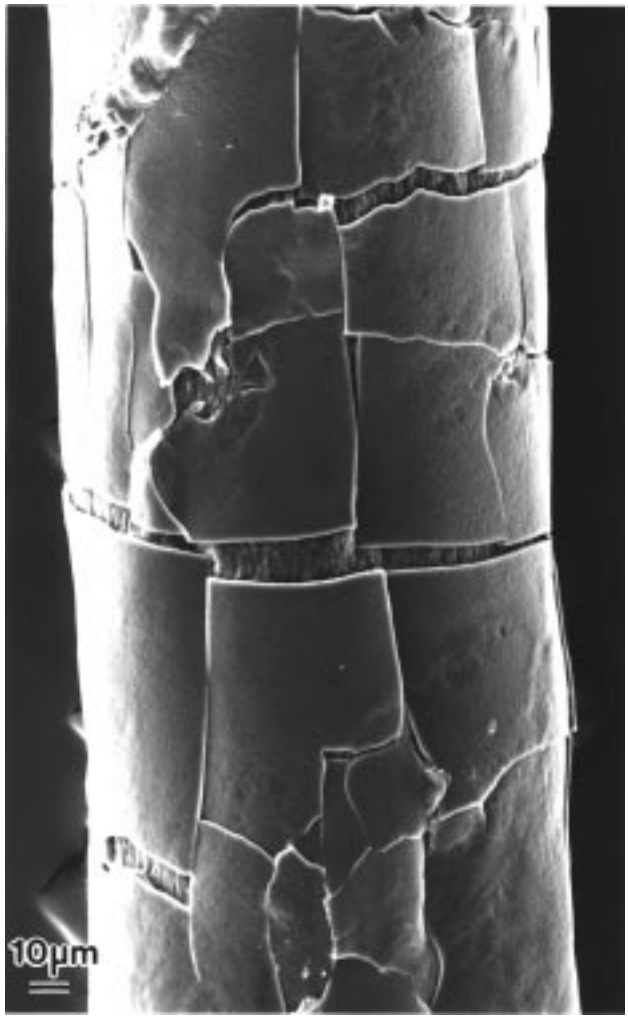

Figure 12. SEM image of the surface of a bacterial−titania composite fiber.

When the bacterial thread is redrawn from the sol, particles become trapped between or adhere to the multicellular filaments such that they are retained and consolidated within the interfilament spaces on drying. The idealized structure would therefore consist of a well-ordered, close-packed array of uniform diameter bacterial filaments that are separated by an interpenetrating, continuous inorganic phase of uniform thickness. In reality, only small areas within the composite have such an idealized structure, because the superstructure is disordered to some extent by the hydration and air-drying process.[12] This is manifested as a lowering in packing density of the bacterial component and a corresponding reduction in the long-range periodicity. Furthermore, the formation of a continuous wall structure requires particle−particle aggregation and fusion into an extended network; although this was observed for amorphous silica nanoparticles,[17] the crystalline magnetite domains remain only loosely associated such that calcination of the composite did not produce a stable porous inorganic replica of the bacterial superstructure.

(23) Forder, C.; Armes, S. P.; Simpson, A. W.; Maggiore, C.; Hawley, M. *J. Mater. Chem.* **1993**, *3*, 563.
(24) Mayes, E. M.; Vollrath, F.; Mann, S. *Adv. Mater.* **1998**, *10*, 801.
(25) Baral, S.; Schoen, P *Chem. Mater.* **1993**, *5*, 145.
(26) Chappell, J. S.; Yager, P. *J. Mater. Sci. Lett.* **1992**, *11*, 633.

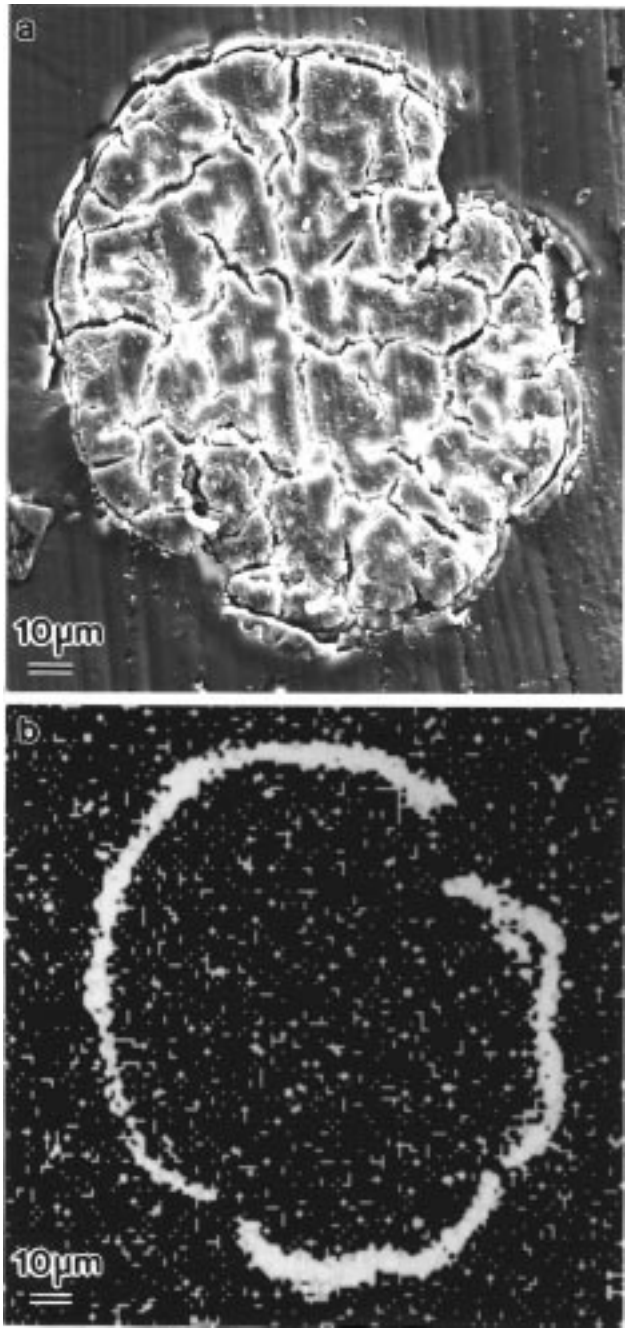

Figure 13. (a) SEM of a bacterial−titania composite embedded in resin and cut perpendicular to the fiber axis. (b) Corresponding Ti distribution map.

In situ deposition of CdS nanoparticles within the bacterial superstructure produced an uneven surface coat with negligible penetration of the thread interior. Swelling of the dry thread in a $CdCl_2$ solution gives rise to partial separation of the multicellular filaments along with strong Cd(II) binding to the highly charged groups present in the bacterial cell wall, which are known to sequester many different metals.[14] To some extent, these interactions disrupt the superstructure, as shown by changes in the surface texture of the threads after air-drying. Subsequent reaction with H_2S gas is diffusion-limited because of the preferential formation of a crust of CdS particles at or near the external surface of the bacterial thread. Although, there is only partial transformation to CdS near the center of the fiber, it should be possible in future experiments to control the diffusion processes to produce fully mineralized CdS−bacterial composites by in situ precipitation.

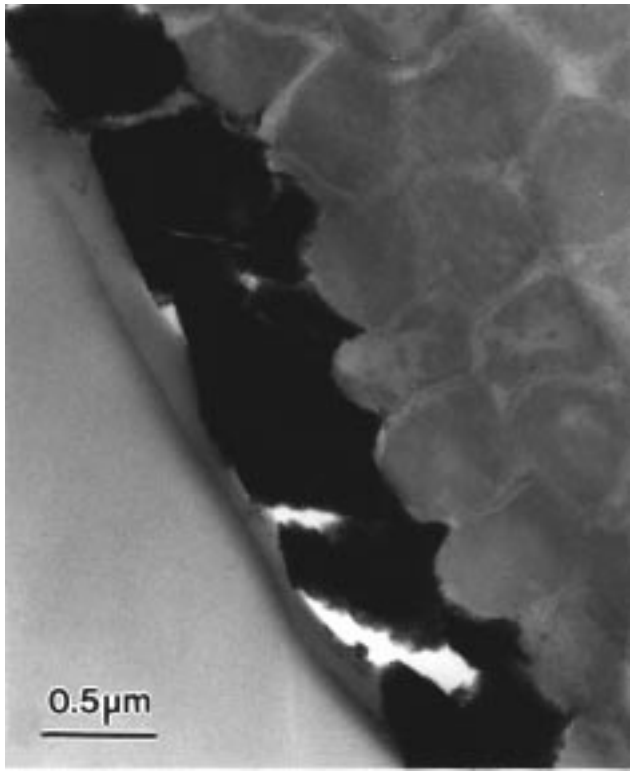

Figure 14. TEM image of a transverse thin section of a bacterial−titania composite fiber showing a uniform consolidated mineral coating at the fiber surface.

Conclusions

The results presented in this paper indicate that bacterial superstructures with reversible swelling properties can be used as 3-D templates for the fabrication of ordered inorganic−organic fibrous composites containing nanoparticles with magnetic (Fe_3O_4) or semiconducting (CdS) properties. Further studies are in progress to establish the optimum conditions for mineral infiltration with different types of inorganic nanoparticles. In the long term, we aim to integrate biotechnological and materials chemistry processes for the fabrication of a wide range of hybrid materials exhibiting patterned microstructures and morphological complexity.

Acknowledgment. We thank BNFL (S.A.D and E.L.M), Leverhulme Trust (S.A.D), EPSRC (H.M.P), the Arizona Agricultural Experimental Station Hatch (N.H.M), and the University of Bath (G.F) for financial support. We also thank K. K. W. Wong for assistance with TEM studies of CdS systems, T. Douglas for help with web cultures and magnetite preparations, and D.J. Riley for helpful discussions.

CM9802853